Bulletin of the Seismological Society of America, Vol. 71, No. 4, pp. 1031–1047, August 1981

ANALYSIS OF SPLIT NORMAL MODES FOR THE 1977 INDONESIAN EARTHQUAKE

BY SETH STEIN AND JEFFREY A. NUNN*

ABSTRACT

The longest period spheroidal mode multiplets, ${}_0S_2$ to ${}_0S_5$, are well recorded on IDA gravimeter records of the 19 August 1977 (M_S 7¾) Indonesian earthquake. We model these modes, which are split into singlets by rotation and ellipticity, using time domain synthetics which reproduce the complex interference pattern between the various singlets in each multiplet. This method, developed to fit a single strainmeter record of the Chilean earthquake, successfully fits records at multiple stations using a common source. We also study the attenuation of the split modes by matching the decay of multiplet envelopes and individual singlets.

INTRODUCTION

The earth's longest period spheroidal mode multiplets are split into individual singlets by the effects of rotation, ellipticity, and lateral heterogeneity. Thus the multiplet spectrum contains a number of individual singlet peaks, each broadened by the effects of attenuation and record length (Benioff *et al.*, 1961; Alsop *et al.*, 1961; Ness *et al.*, 1961). The corresponding time series shows a complicated interference pattern resulting from the beating of the singlets, each with its own amplitude and phase (Stein and Geller, 1977, 1978a).

Theoretical results for the eigenfrequencies of the split singlets have been given by Pekeris *et al.* (1961) and Backus and Gilbert (1961) for the effects of rotation, and by Dahlen (1968) and Dahlen and Sailor (1979) for rotation and ellipticity. Theoretical results for the amplitudes of the split mode singlets were obtained by Stein and Geller (1977) and Geller and Stein (1977).

The major limitation on studies of these longest period modes has been a shortage of data. Until recently, the Isabella strainmeter record of the 1960 Chilean earthquake and the UCLA gravimeter record of the 1964 Alaskan earthquake were the only two records adequate for the study of ${}_0S_2$ to ${}_0S_5$. As a result, these two records became among the most heavily analyzed of geophysical time series.

The 19 August 1977 (M_S 7¾) Indonesian earthquake, recorded on the ultra-long period gravimeters of the IDA network (Agnew *et al.*, 1976) provided a new dataset for the longest period modes. In particular, this data provided records of a single earthquake at seven stations: such multiple coverage in this frequency range had not been previously available. The data has already been used for studies of the attenuation of the unsplit modes (Geller and Stein, 1979; Stein *et al.*, 1981; Buland, 1981; Sleep *et al.*, 1981), for the attenuation of ${}_0S_0$ (Reidesel *et al.*, 1980) and for source mechanism inversion (Kanamori, 1980; Chou and Dziewonski, 1980). Splitting parameters for ${}_0S_2$ and ${}_0S_3$ have been obtained from the IDA records by Buland *et al.* (1979).

The purpose of this study is to apply the time domain analysis method developed by Stein and Geller (1977, 1978a) to the Indonesia records. This technique had been previously applied to single records of the Chilean and Alaskan earthquakes. The

* Present address: Department of Geology, Louisiana State University, Baton Rouge, Louisiana 70803.

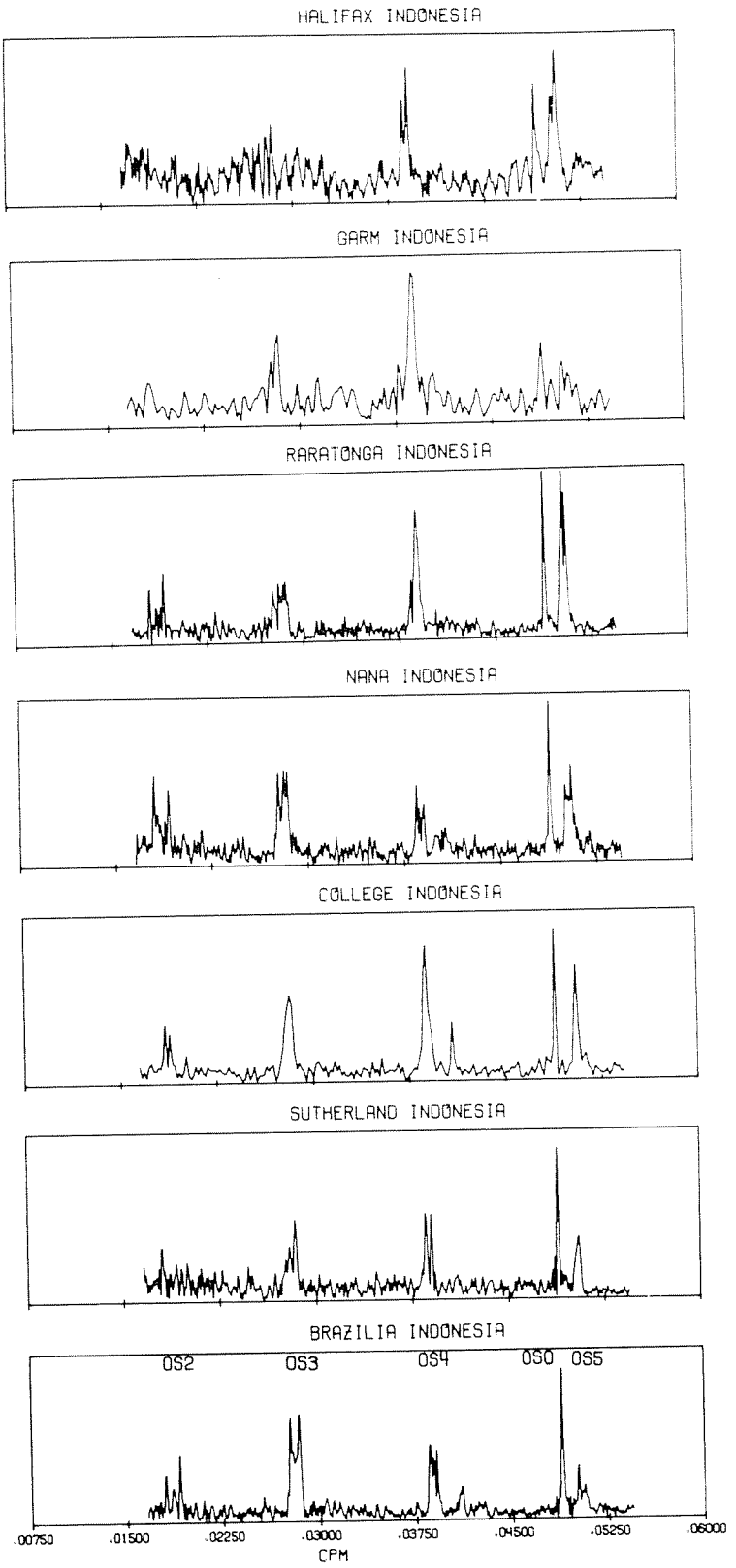

FIG. 1. Long-period spectra at seven IDA stations showing split modes ${}_0S_2$ to ${}_0S_5$.

natural next step is to apply it to multiple records of a single event, and show that they can be fit simultaneously using the same source. After successfully fitting the records, we then use this method to estimate the attenuation of these modes.

DATA

Seven IDA stations recorded the Indonesian earthquake: Nana, Peru (NNA); Halifax, Nova Scotia (HAL); College, Alaska (CMO); Sutherland, South Africa (SUR); Raratonga, Cook Islands (RAR); Brazilia, Brazil (BDF); and Garm, USSR (GAR). The records and processing used are those used by Geller and Stein (1979) except that the data were not decimated. The earliest portions (up to 30 hr) of each record were deleted to avoid the saturation due to large amplitude surface waves; the solid earth tide was removed by twice subtracting a $1\frac{1}{2}$-hr running average from the data. Two stations had shorter record lengths than the others: at GAR due to long-period noise from the flooding of a nearby river, and at SUR due to the rezeroing of the instrument mass.

Figure 1 shows the longest period portion of the spectrum at each station. The signal to noise of various modes differs from station to station. For example, ${}_0S_2$ is not as well recorded at any station as it was on the Chile and Alaska records. ${}_0S_4$, on the other hand, is well recorded at all seven stations; ${}_0S_3$ is well recorded at most stations, but not at HAL, for example. Splitting is clearly visible for most of the multiplets.

To model the data, we use the results of Stein and Geller (1977) for the amplitudes of the split normal mode singlets excited by a double couple source. The solution is obtained by transforming the spherical harmonic expansion of the displacement from the frame of reference of the earthquake source into the geographic frame which yields the observed split modes. The singlet amplitudes depend on source location, source depth, fault geometry, and receiver location. For a source we used parameters derived by Kanamori (personal communication): $\phi_f = 270°$; $\delta = 45°$; $\lambda = -74°$. The resulting excitation in geographic coordinates is shown in Figure 2 for the ${}_0S_4$ and ${}_0S_3$ multiplets.

In the geographic coordinate frame, all $2l + 1$ or nine singlets are excited, rather than the -2 to $+2$ singlets which are excited in the source frame. The excitation differs dramatically from station to station, as can be seen by comparing, e.g., CMO and NNA. The spectra shown are displacement, for which expressions are given by Stein and Geller (1977); the relation between vertical displacement and the gravimeter records is discussed in an Appendix. The amplitudes of the $-m$ and $+m$ singlets are equal since the source is a point source. (Previous numerical experiments for the Chilean earthquake, using a 1000-km fault length, showed almost no difference from the point source results.)

Figure 3 shows the theoretical spectral amplitude of the largest singlet in each multiplet at each station. These results generally agree with those expected from the spectra (Figure 1): e.g., ${}_0S_2$ is best seen at NNA, BDF, and RAR. It is interesting to note that the poor signal for ${}_0S_2$ at SUR and GAR is not due to the short-record lengths analyzed—the mode is simply not well excited at those stations. Finally, as the figure shows the maximum singlet excitation, direct comparison between different modes at the same station can be misleading because the number of singlets (and thus total energy) varies between modes, and because of interference between singlets.

The seismograms were synthesized in the time domain, so that all the processing

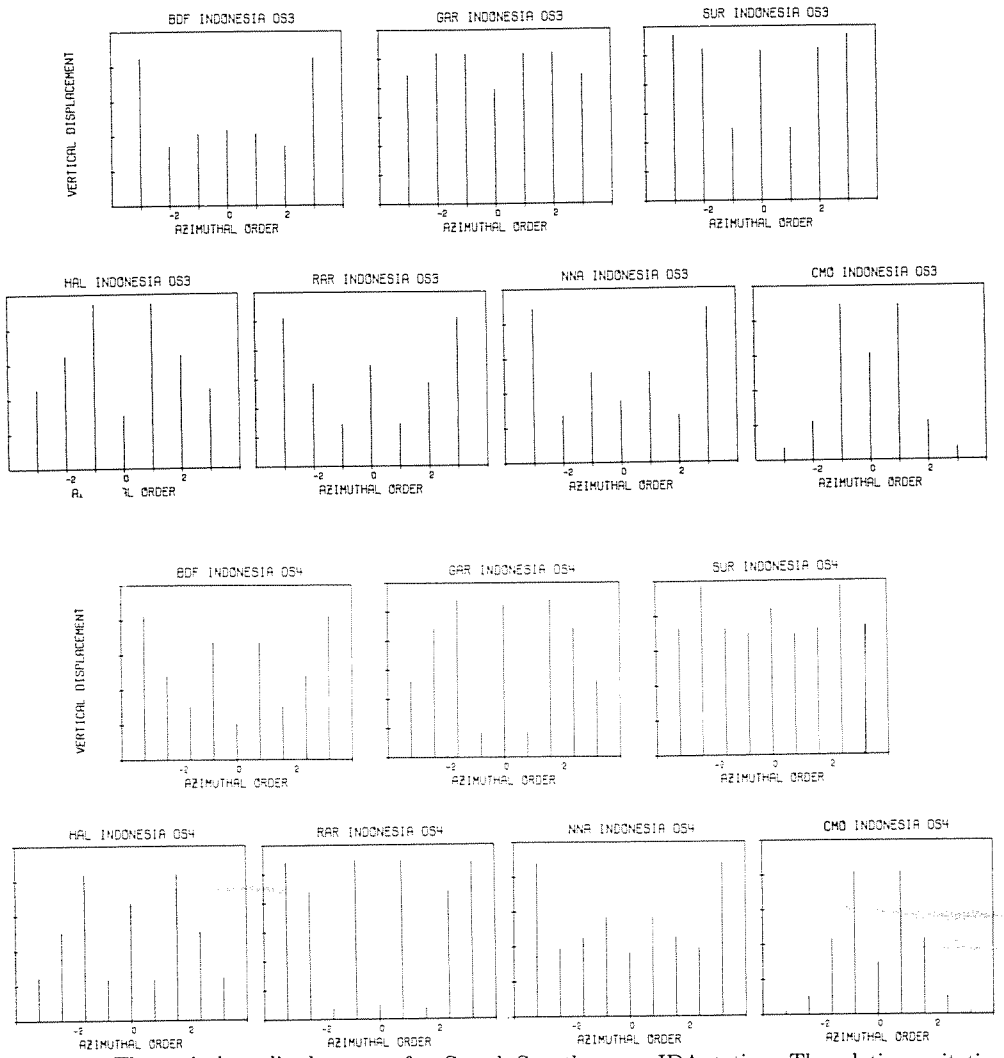

FIG. 2. Theoretical amplitude spectra for ${}_0S_3$ and ${}_0S_4$ at the seven IDA stations. The relative excitation differs significantly from station to station.

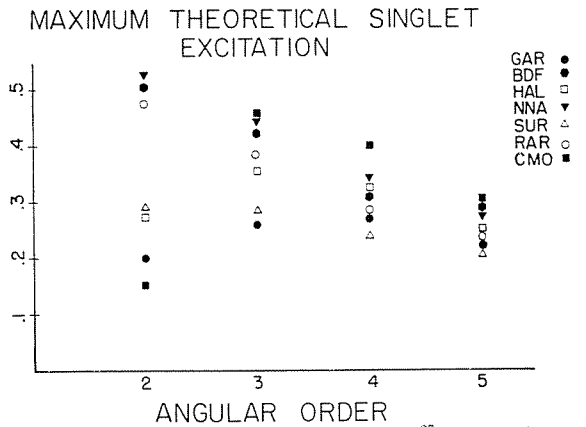

FIG. 3. Theoretical amplitude (in 10^{-4} cm ground motion/10^{27} of seismic moment) of the largest singlet in each multiplet at different stations.

used on the data could be applied to the synthetics. Before examining the results, it is useful to consider the same process in the frequency domain. Figure 4 shows data for the ${}_0S_2$ multiplet at Brazilia: the ±2 and 0 singlets are best excited. The synthetic amplitude spectrum is shown: first without the effects of attenuation and record length; next including attenuation ($Q = 500$), which produces the characteristic resonance curves; and finally including the effect of record length, giving rise to $(\sin x)/x$-type spectra, broadened and with side lobes. It is clear that record length as well as attenuation have major effects on the spectrum and time series. These effects are included naturally in the time domain synthetics. The agreement between synthetic and observed spectra (and thus the resulting time series) is good but not perfect, due to any one of a number of noise effects.

Synthetic Seismograms

To analyze the data, modes with adequate spectral amplitudes were narrow band-filtered to isolate a single multiplet. Synthetic seismograms were then synthesized, tapered, and bandpassed in exactly the same way as the data. The results are shown in Figures 5 to 8.

${}_0S_4$ (Figure 5) is the best sample; it was well excited at all seven stations. The excitation (Figure 2) and thus singlet interference pattern differ substantially between stations. This, then, provides an excellent test for our time domain synthesis method. The synthetics agree extremely well with data in terms of maximum and minimum times and of amplitude decay.

${}_0S_3$ (Figure 6) yields excellent results at five stations: ${}_0S_5$ does well (Figure 7) at two (RAR and HAL). ${}_0S_2$ is fit adaquately, although not as well as the other modes at four stations (Figure 8) The difficulties with ${}_0S_2$ appear to be due to the size of the earthquake: its moment (3×10^{28} dyne-cm; Kanamori, personal communication) is substantially less than that of the Chilean or Alaskan earthquakes. A variety of experiments designed to improve the results for ${}_0S_2$ had no noticeable effects. This is not due to inaccurate splitting parameters: those used (Dahlen and Sailor, 1979) agree well with the observed eigenfrequencies (Buland *et al.*, 1979). Unfortunately, a signal-to-noise ratio adequate for eigenfrequency determination is not necessarily adequate for stable amplitude studies.

Attenuation

The Q_S of the longest period spheroidal modes, ${}_0S_2$ to ${}_0S_5$, form the best constraint on the attenuation structure of the lowermost mantle, due to the depths sampled by their kernals (Sailor, 1978; Sailor and Dziewonski, 1978; Stein *et al.*, 1981; Nakanishi, 1981). At present, measurements of these Q_S scatter considerably, as discussed by Stein and Geller (1978b). As a result, lower mantle Q structure is poorly constrained (Stein *et al.*, 1981).

It is difficult to measure these Q_S, primarily because only the very largest earthquakes provide sufficiently large amplitudes at these long periods. Only the Chilean and Alaskan data have to date been usable: considerable scatter occurs from the use of different techniques on the same dataset. The Indonesian earthquake is considerably smaller, but the data quality is higher, so we attempted to measure Q for the longest period modes.

Comparison of theoretical multiplet beat patterns with data provides a method of measuring the attenuation of split modes which minimizes the difficulties introduced

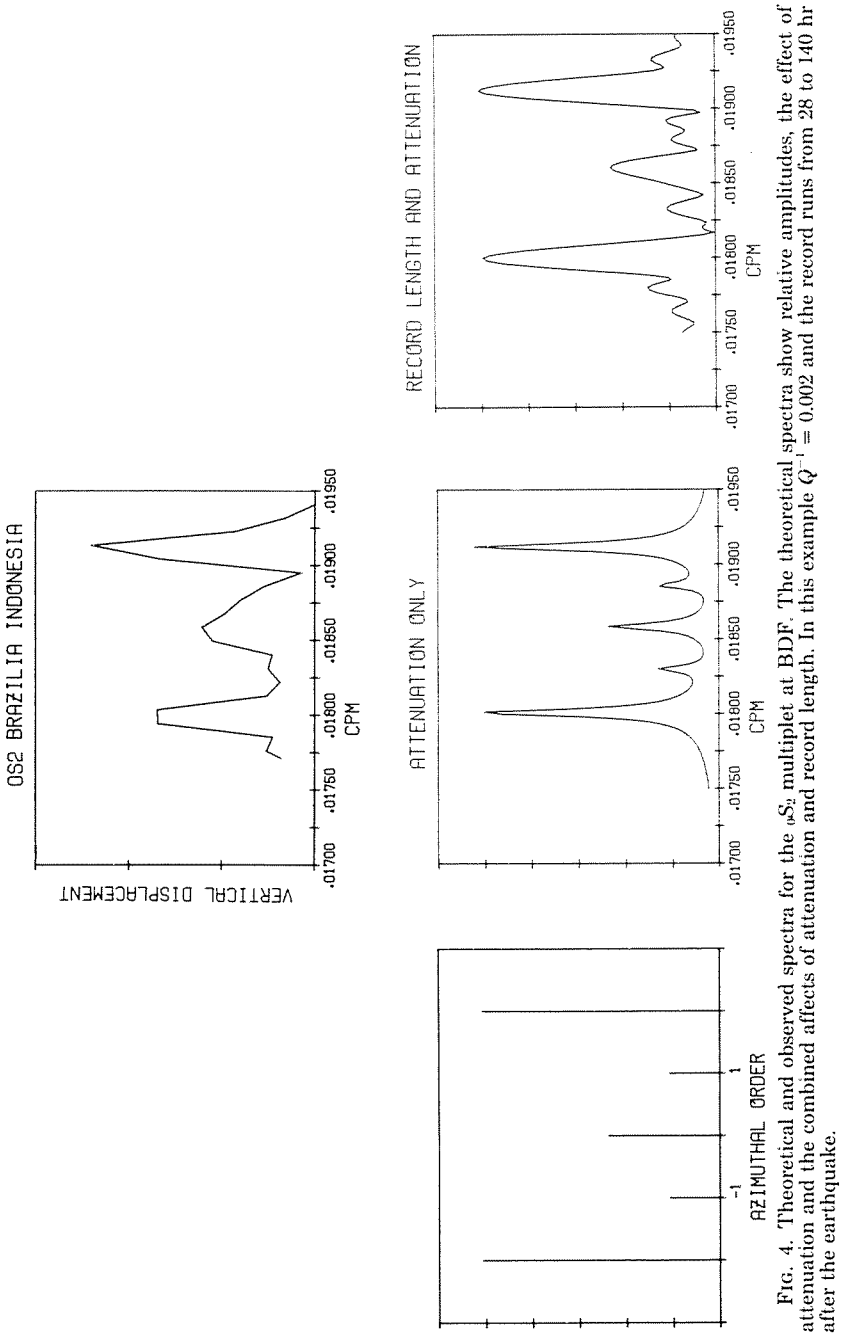

FIG. 4. Theoretical and observed spectra for the ${}_0S_2$ multiplet at BDF. The theoretical spectra show relative amplitudes, the effect of attenuation and the combined affects of attenuation and record length. In this example $Q^{-1} = 0.002$ and the record runs from 28 to 140 hr after the earthquake.

FIG. 4. Theoretical and observed spectra for the ${}_0S_2$ multiplet at BDF. The theoretical spectra show relative amplitudes, the effect of attenuation and the combined affects of attenuation and record length. In this example $Q^{-1} = 0.002$ and the record runs from 28 to 140 hr after the earthquake.

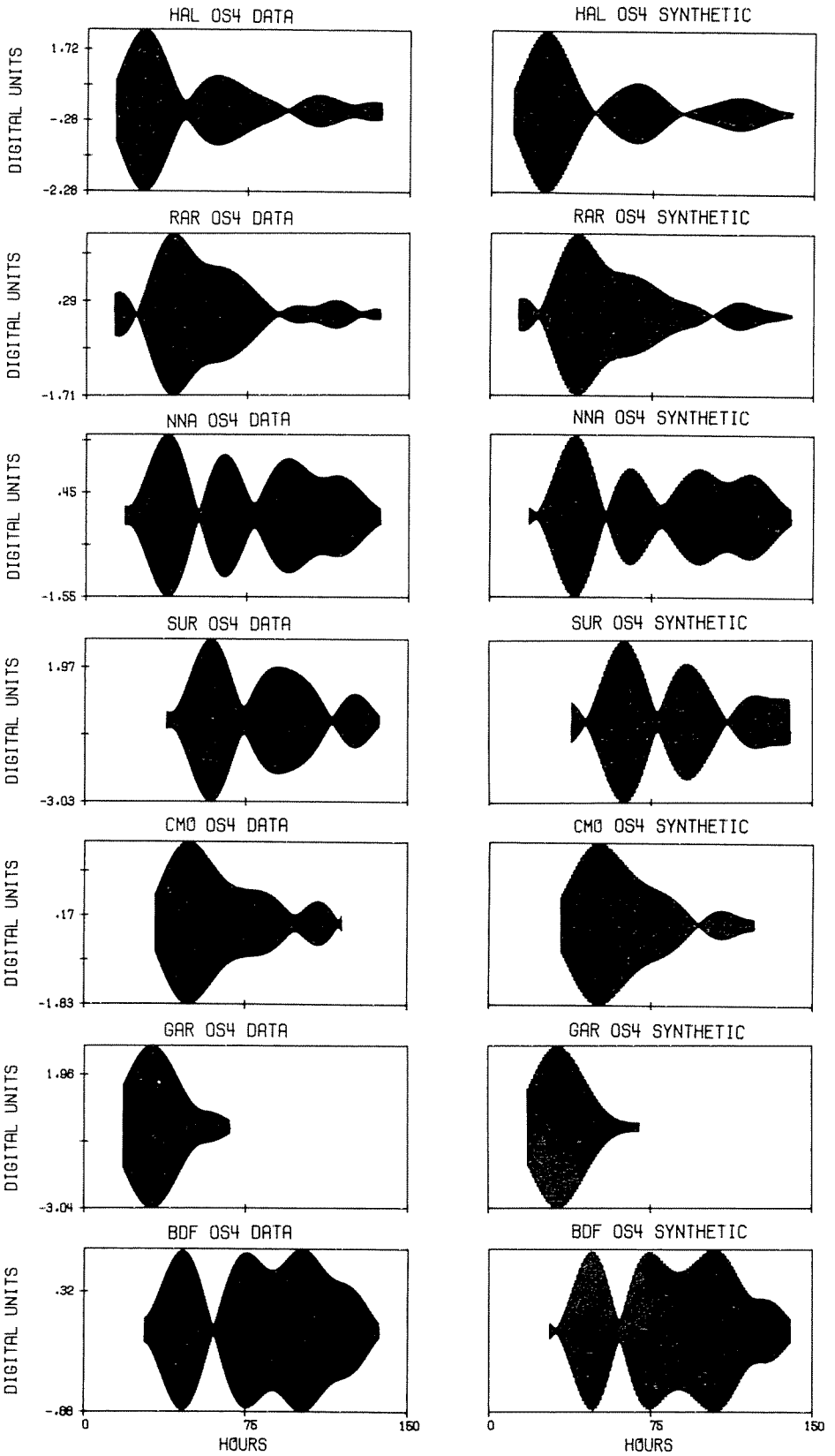

FIG. 5. Observed and synthetic multiplet time series for ${}_0S_4$. $Q^{-1} = 0.0025$ was used for all synthetics.

by the splitting (Stein and Geller, 1978b). In this procedure we form the Hilbert transform envelope of data and synthetics, and smooth each with a 50-hr running average for ease of comparison. By comparing the data to synthetics generated with a range of values of Q^{-1}, a best-fitting value can be obtained.

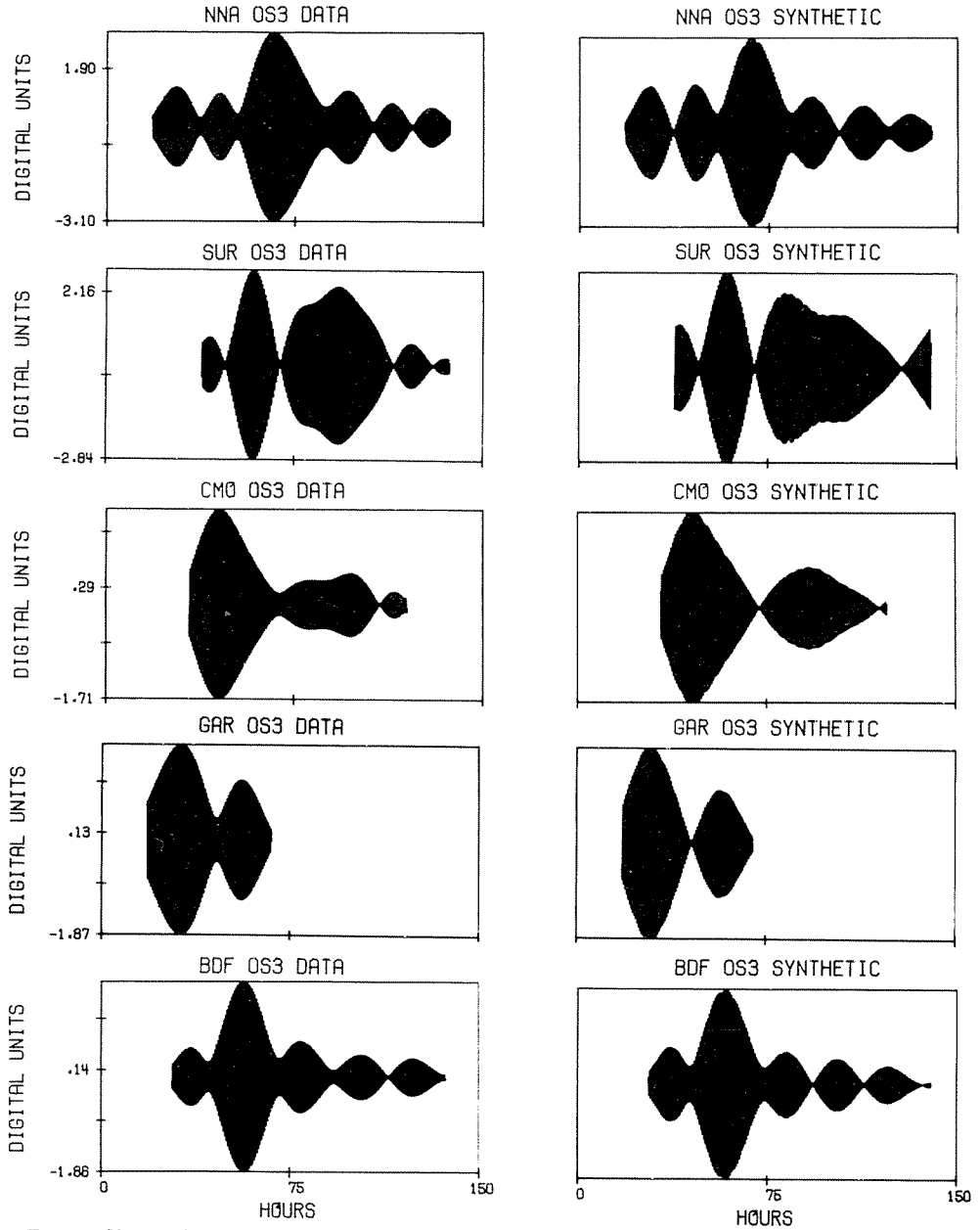

FIG. 6. Observed and synthetic multiplet time series for ${}_0S_3$. $Q^{-1} = 0.002$ was used for all synthetics.

Figure 9 shows the results for ${}_0S_4$ at the best five stations. Dashed lines are the data and solid lines are synthetics, corresponding to the indicated values of Q^{-1}. Several of the stations—HAL, BDF, and NNA—show extremely stable measurements with Q^{-1} between 0.003 and 0.002 (Q from 333 to 500).

Figure 10 shows similar results for ${}_0S_3$ and ${}_0S_2$. As expected from our earlier discussion, the values for ${}_0S_3$ are substantially better than those for ${}_0S_2$, which show serious noise effects.

An alternative to examining the decay of an entire multiplet is to study an individual singlet. In general, this is rather difficult, as individual singlets are not well resolved in the data. Naturally, singlets are best resolved under the fortuitous circumstance that the "outermost", i.e., $m = \pm l$ singlets are much better excited than the adjacent ones. By predicting the relative excitation of singlets at each station, we can determine stations at which narrow-band filtering for singlets is most likely to be successful.

Figure 2, showing the theoretical relative amplitudes of the ${}_0S_3$ multiplet, indicates that the best isolated ±3 singlets occur at BDF and NNA. At the other stations, e.g., CMO, isolating a single singlet is much more difficult because of the relative amplitudes. This occurs despite the fact that the overall multiplet signals are quite good and very well modeled by the synthetics.

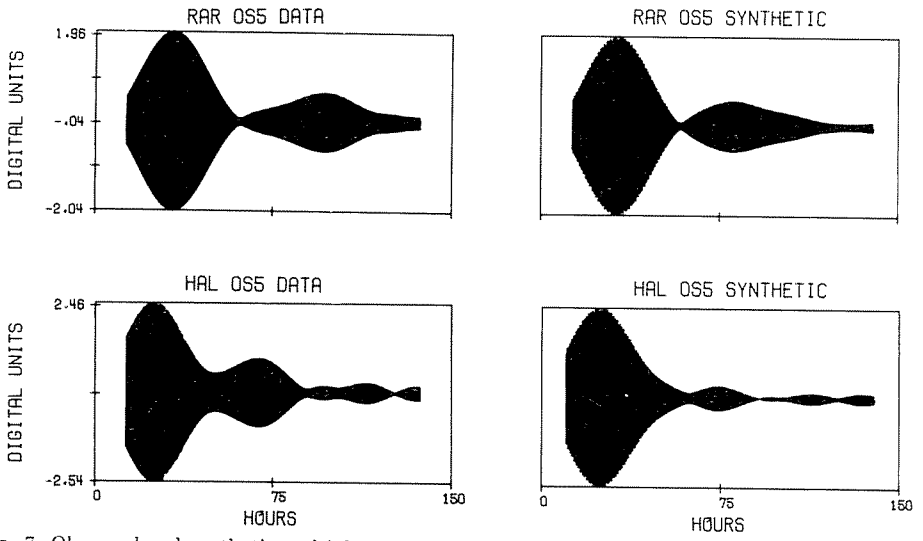

FIG. 7. Observed and synthetic multiplet time series for ${}_0S_2$. $Q^{-1} = 0.0015$ was used for all synthetics.

Figure 11 shows amplitude decay curves for four ${}_0S_3$ singlets; two at BDF and two at NNA. The smooth curves on the logarithmic amplitude plot indicate that the singlets are relatively free of noise, which would yield a scalloped decay curve (Geller and Stein, 1979). The data, although adequate, is not as good as for the shorter period multiplets used by Geller and Stein (1979). A least-squares line was fit to the segment of the data from the peak amplitude until the time the signal decayed to e^{-1} of the peak value. Q^{-1} was then computed from the slope of the line. The nominal error bars, from the standard least-squares formula, are only a few per cent, but these errors are considered to seriously underestimate the true uncertainties (Geller and Stein, 1979). More realistic estimates can be derived from the differences between measurements.

Figure 12 shows the best singlet amplitude data for ${}_0S_4$. The +4 singlet at BDF did not yield stable results. Similar efforts to measure singlet decay for ${}_0S_2$ at BDF, RAR, NNA were unsuccessful: although the amplitude spectrum showed well isolated peaks, the decay curves showed serious scalloping. This is unfortunate as the Q^{-1} of ${}_0S_2$ is quite important for lower mantle attenuation structure.

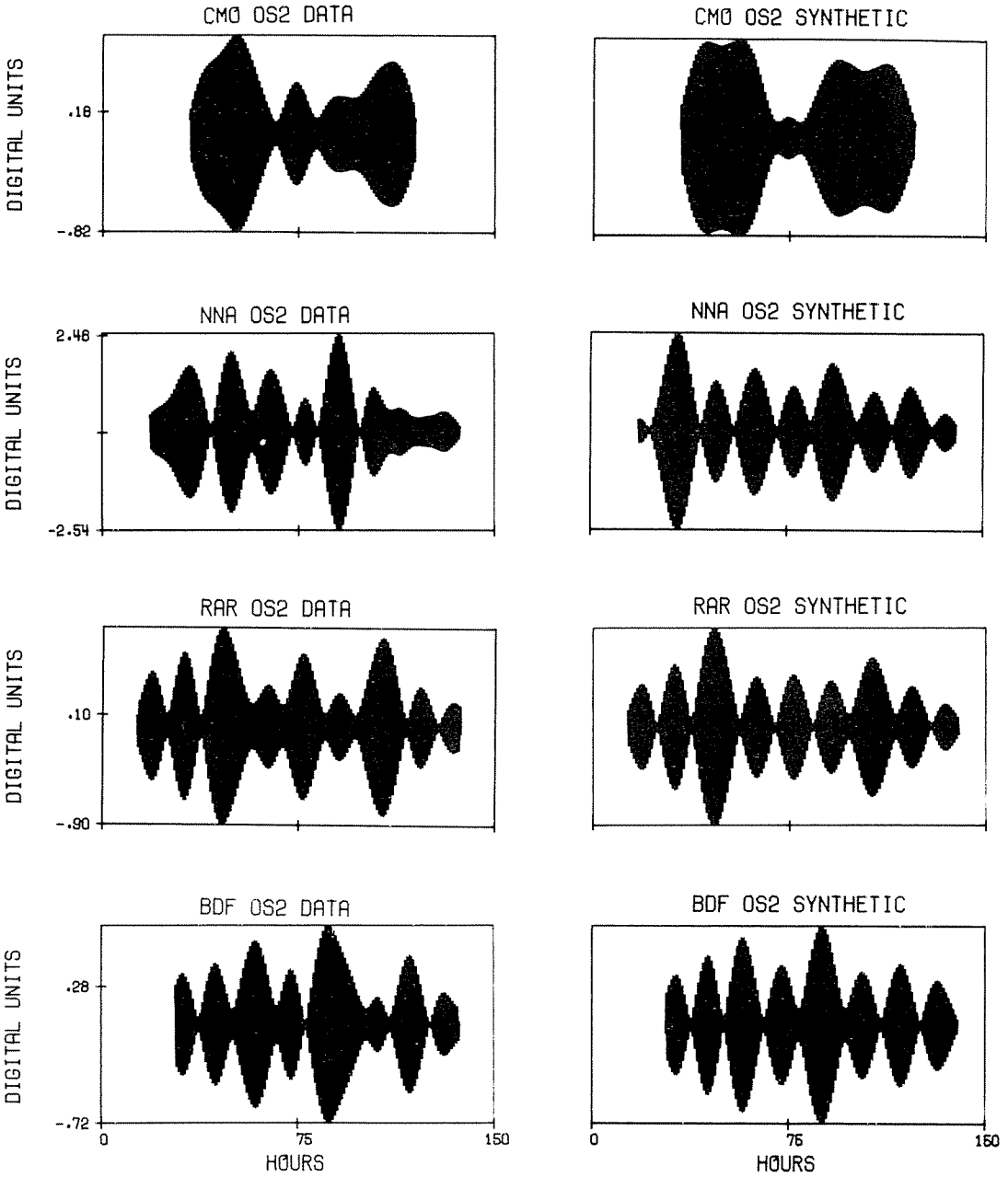

FIG. 8. Observed and synthetic multiplet time series for ${}_0S_5$. $Q^{-1} = 0.004$ was used for all synthetics.

The combined singlet and multiplet attenuation results for ${}_0S_3$ and ${}_0S_4$ are summarized in Figure 13. With the present data alone, it seems most prudent to regard the differences between individual multiplet measurements, individual singlet measurements, and the multiplet and singlet measurements as a measure of the uncertainty in our knowledge of the attenuation of these two modes.

Also shown are the results of previous studies using the data from the Chilean

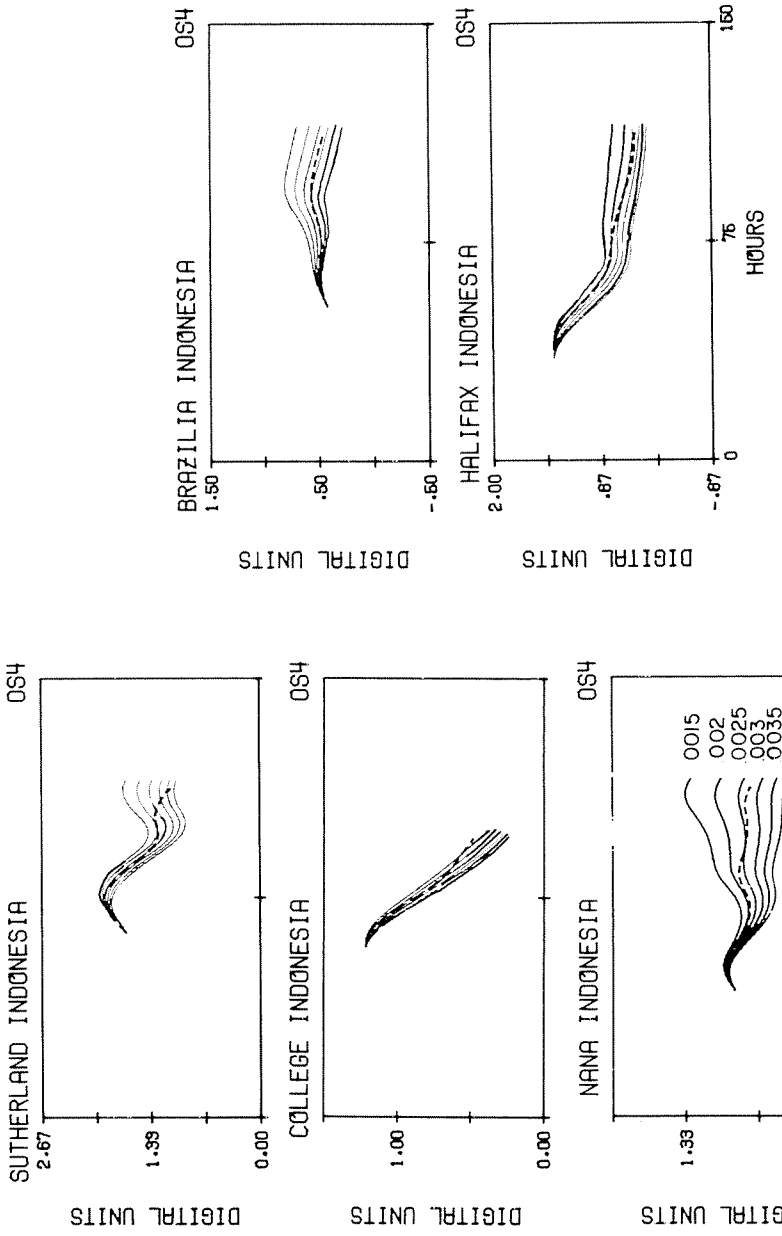

FIG. 9. Hilbert transform envelopes of the observed (dashed line) and synthetic multiplet time series for ${}_0S_4$.

SYNTHETIC

SYNTHETIC

SYNTHETIC

SYNTHETIC

5 150

RS

all synthetics.

and ${}_0S_4$ are
st prudent to
vidual singlet
easure of the

the Chilean

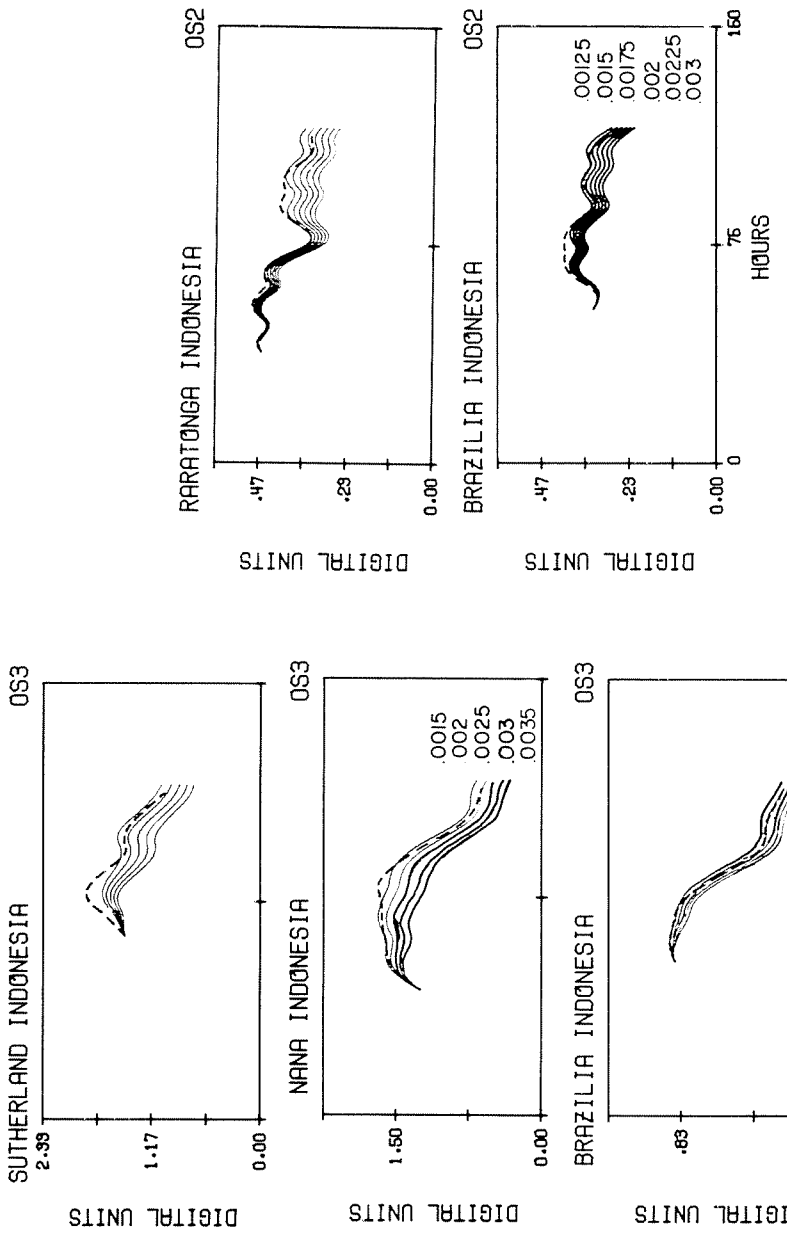

FIG. 10. Hilbert transform envelopes for ${}_0S_3$ and ${}_0S_2$ multiplets.

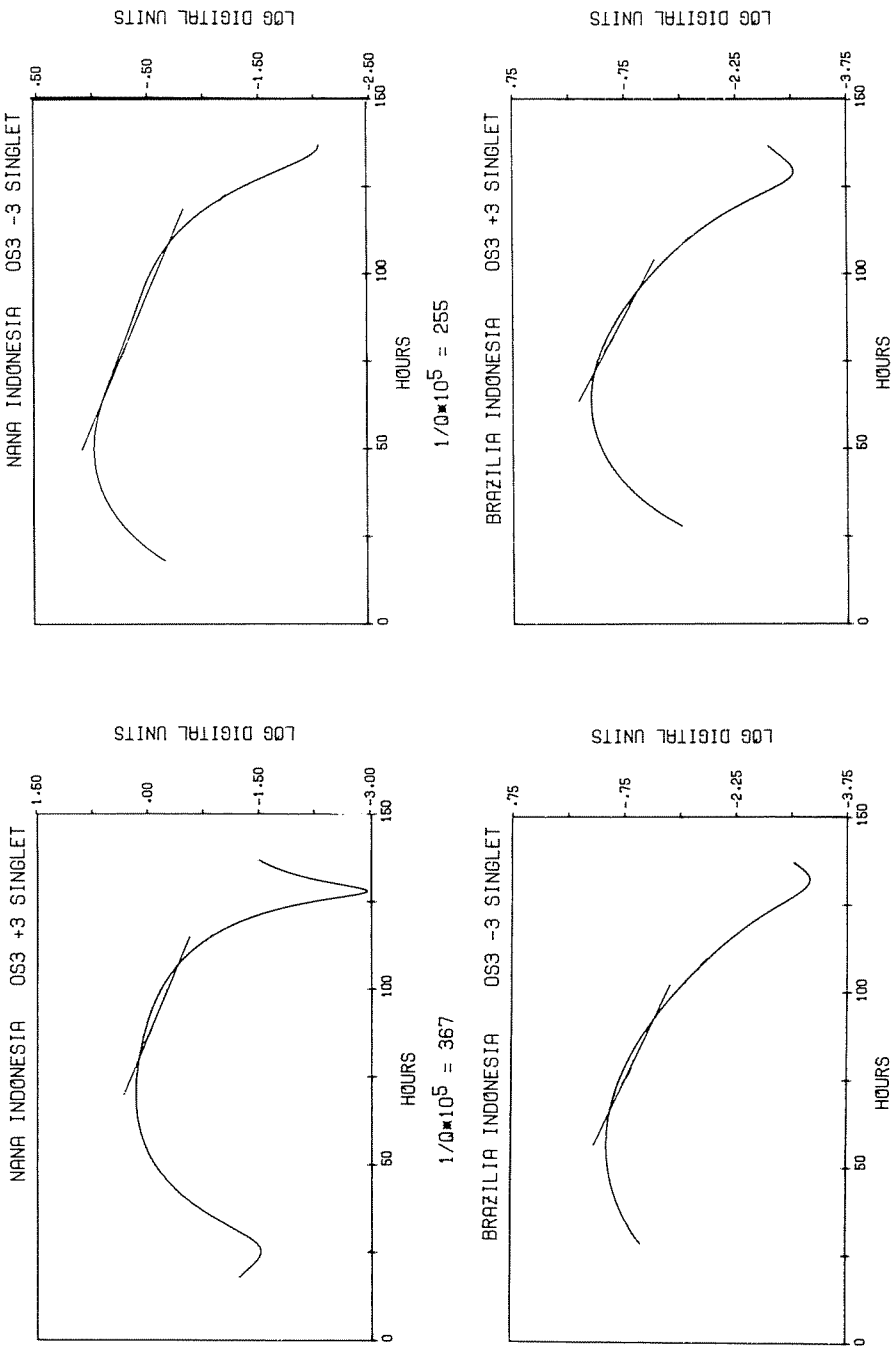

FIG. 11. Amplitude decay plots and best-fitting least-squares lines for ${}_0S_3$ at BDF and NNA.

160

7b

HOURS

FIG. 10. Hilbert transform envelopes for ${}_0S_3$ and ${}_0S_2$ multiplets.

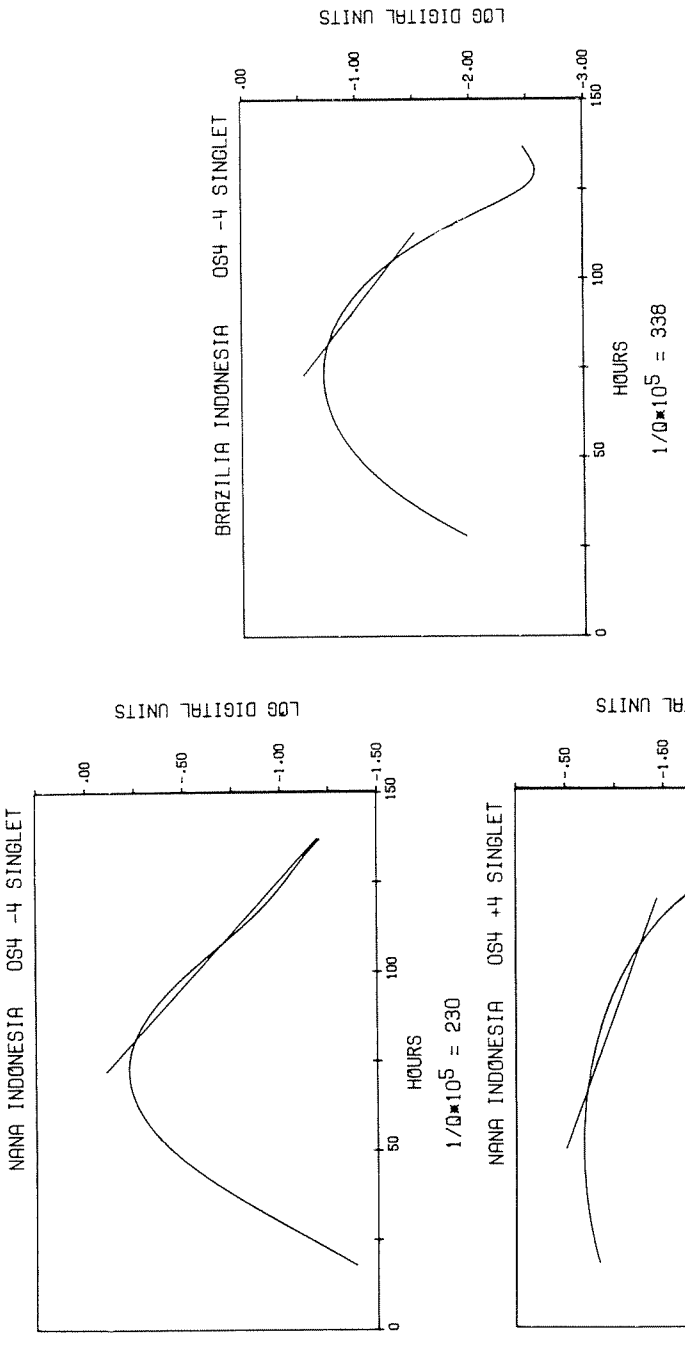

FIG. 12. Amplitude decay plots and best-fitting least-squares lines for ${}_0S_3$.

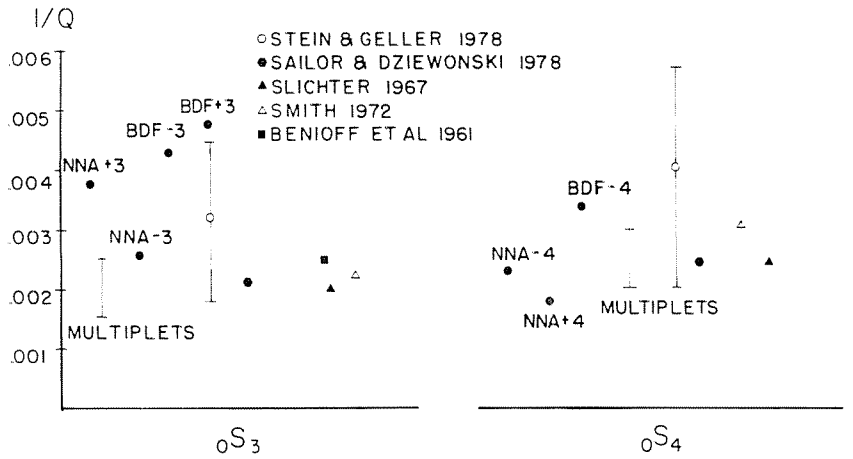

FIG. 13. Comparison of attenuation measurements for ${}_0S_3$ and ${}_0S_4$.

(Benioff *et al.*, 1961), Alaskan (Slichter, 1967; Sailor and Dziewonski, 1978), or both (Smith, 1972; Stein and Geller, 1978), earthquakes. The results of this study are generally similar to those of the previous studies. This is quite encouraging in that it is important to establish the uncertainty in values for Q, since the uncertainty can be explicitly included in inversions. The formal uncertainties in a single Q measurement probably underestimate the true uncertainties; which are better established by multiple independent measurements using as wide a range of analysis techniques as possible. Each type of measurement has its own uncertainty. The plus and minus singlets at a single station, which should have identical Q_S, give the minimum scatter. Greater scatter occurs between the same singlets at different stations, which should also have the same Q. There are many possible sources of uncertainty in the time domain synthesis, some of which are discussed in the Appendix. Other uncertainties include lateral heterogeneity, either in velocity or in Q (Sleep *et al.*, 1981), which can cause either real or apparent differences between singlets, and affect the multiplet results. Clearly a major improvement, as well as better data for ${}_0S_2$, will require IDA records of a significantly larger earthquake.

FIG. 12. Amplitude decay plots and best-fitting least-squares lines for ${}_0S_3$.

CONCLUSIONS

The results of our analysis show that the split modes can be very well modeled by calculating the excitation of the individual singlets in the multiplet. Time domain synthetics successfully reproduce strikingly different records observed at the individual stations. The envelopes of the data can be used to study the attenuation of the multiplet. Furthermore, the theoretical excitation can be used to identify individual singlets which can be used for attenuation studies. When IDA data for earthquakes larger than the Indonesian event become available, these methods should yield even better results.

APPENDIX

The vertical component of displacement for a multiplet of angular order l can be written

$$U(t) = \sum_{m=-l}^{l} (E_{lm} e^{i\omega_{lm} t} + E_{lm}^{*} e^{-i\omega_{lm} t}) e^{-\omega_{lm} t/2Q_{lm}}$$

or

$$U(t) = \sum_{m=-l}^{l} \{2\mathrm{Re}(E_{lm}) \cos \omega_{lm} t - 2\mathrm{Im}(E_{lm}) \sin \omega_{lm} t\} e^{-\omega_{lm} t/2Q_{lm}}$$

where E_{lm} is the value at the earth's surface of the radial component of the $E_{lm}(r)$ vector (Stein and Geller, 1977).

The corresponding acceleration is then

$$\ddot{U}(t) = \sum_{m=-l}^{l} (-\omega_{lm}^2) \{2\mathrm{Re}(Z_{lm}) \cos \omega_{lm} t - 2\mathrm{Im}(Z_{lm}) \sin \omega_{lm} t\} e^{-\omega_{lm} t/2Q_{lm}}$$

where

$$\mathrm{Re}(Z_{lm}) = \mathrm{Re}(E_{lm}) \left(1 - \frac{1}{4Q_{lm}^2}\right) - \frac{\mathrm{Im}(E_{lm})}{Q_{lm}}$$

and

$$\mathrm{Im}(Z_{lm}) = \mathrm{Im}(E_{lm}) \left(1 - \frac{1}{4Q_{lm}^2}\right) + \frac{\mathrm{Re}(E_{lm})}{Q_{lm}}.$$

For the modes in question, Q is approximately 300, so corrections of order $1/Q$ and $1/Q^2$ may be neglected, and the acceleration amplitudes Z_{lm} can be taken equal to the displacement amplitudes E_{lm}.

A second effect is the factor $-\omega_{lm}^2$, which differs from singlet to singlet. The maximum possible frequency difference occurs for the $-l$ and l singlets in each multiplet. For ${}_0S_3$, the ratio $(\omega_{33}^2/\omega_{3-3}^2)$ is approximately 1.06, so any effect will be negligible, especially compared to the noise in the data. Numerical experiments in which multiplets were synthesized with and without this factor were indistinguishable.

An additional effect is that the gravimeter measures acceleration and changes in the gravity field. Okal (1981) has calculated the magnitude of this effect and showed that it is less than 5 per cent for ${}_0S_5$ to ${}_0S_3$, and approximately 9 per cent for ${}_0S_2$. It has therefore been neglected in these calculations.

The synthetic spectra (Figures 2 and 4) and time series (Figures 5 to 8) were thus calculated for the vertical component of displacement. In a further simplification (for computational purposes) Q, rather than the formally correct Q_{lm}/ω_{lm} for a spherically symmetric structure was assumed constant for the multiplet. Finally, as discussed earlier, a point source approximation, justified for these extremely long-period modes, was used in calculating the excitation.

The agreement between the theoretical and observed seismograms suggests that these approximations are justified relative to the noise level in the data.

Acknowledgments

We thank Robert Geller, Hiroo Kanamori, Emile Okal, and Norman Sleep for useful discussions. We also thank Ray Buland and Freeman Gilbert for providing us with the IDA data and information about the records. This work was supported by NSF Grant EAR 80-07363.

References

Agnew, D., J. Berger, R. Buland, W. Farrell, and F. Gilbert (1976). International deployment of accelerometers: a network for very long period seismology, *EOS, Trans. Am. Geophys. Union* **57,** 180–188.

Alsop, L. E., G. Sutton, and M. Ewing (1961). Free oscillations of the earth observed on strain and pendulum seismographs, *J. Geophys. Res.* **66,** 631–641.

Backus, G. and F. Gilbert (1961). The rotational splitting of the free oscillations of the earth, *Proc. Natl. Acad. Sci. USA* **47,** 362–371.

Benioff, H., F. Press, and S. Smith (1961). Excitation of the free oscillations of the earth, *J. Geophys. Res.* **66,** 605–619.

Buland, R. (1981). On interference among free oscillations of the earth, *Geophys. J.* (in press).

Buland, R., J. Berger, and F. Gilbert (1979). Observations of attenuation and splitting from the IDA network, *Nature* **277,** 358–362.

Chou, T. and A. M. Dziewonski (1980). Simultaneous determination of the seismic moment tensor and hypocentral parameters (abstract), *EOS, Trans. Am. Geophys. Union* **61,** 296.

Dahlen, F. A. (1968). The normal modes of a rotating elliptical earth, *Geophys. J.* **16,** 329–367.

Dahlen, F. A. and R. V. Sailor (1979). Rotational and elliptical splitting of the free oscillations of the earth, *Geophys. J.* **58,** 609–624.

Geller, R. J. and S. Stein (1977). Split free oscillation amplitudes for the 1960 Chilean and 1964 Alaskan earthquakes, *Bull. Seism. Soc. Am.* **67,** 651–660.

Geller, R. J. and S. Stein (1979). Time domain attenuation measurements ($_0S_6$ to $_0S_{28}$) for the 1977 Indonesian earthquake, *Bull. Seism. Soc. Am.* **69,** 1671–1691.

Kanamori, H. (1980). Use of the IDA network for fast determination of earthquake source parameters (abstract), *EOS, Trans. Am. Geophys. Union* **61,** 296.

Nakanishi, I. (1981). Shear velocity and shear attenuation models inverted from the worldwide and pure-path average data of mantle Rayleigh waves ($_0S_{25}$–$_0S_{80}$) and fundamental spheroidal modes ($_0S_2$–$_0S_{24}$), *Geophys. J.* (in press).

Ness, N., J. Harrison, and L. Slichter, (1961). Observations of the free oscillations of the earth, *J. Geophys. Res.* **66,** 621–629.

Okal, E. A. (1981). On the importance of changes in the gravity field on seismic recording at ultralong periods, *Proc. Natl. Acad. Sci.* **78,** 20–21.

Pekeris, C. L., Z. Alterman, and H. Jarosch (1961). Rotational multiplets in the spectrum of the earth, *Phys. Rev.* **122,** 1692–1700.

Riedesel, M., D. Agnew, J. Berger, and F. Gilbert (1980). Stacking for the frequencies and Q_S of $_0S_0$ and $_1S_0$, *Geophys. J.* **62,** 457–472.

Sailor, R. V. (1978). Attenuation of low frequency seismic energy, *Ph.D. Thesis*, Harvard University, Cambridge.

Sailor, R. V. and A. M. Dziewonski (1978). Measurements and interpretation of normal mode attenuation, *Geophys. J.* **53,** 559–582.

Slichter, L. B. (1967). Spherical oscillations of the earth, *Geophys. J.* **14,** 171–177.

Smith, S. W. (1972). The anelasticity of the mantle, *Tectonophysics* **13,** 601–622.

Stein, S. and R. J. Geller (1977). Amplitudes of the split normal modes of a rotating, elliptical earth excited by a double couple, *J. Phys. Earth* **25,** 117–142.

Stein, S. and R. J. Geller (1978a). Time domain observations and synthesis of split spheroidal and torsional free oscillations of the 1960 Chilean earthquake: preliminary results, *Bull. Seism. Soc. Am.* **68,** 325–332.

Stein, S. and R. J. Geller (1978b). Attenuation measurements of split normal modes for the 1960 Chilean and 1964 Alaskan earthquakes, *Bull. Seism. Soc. Am.* **68,** 1595–1611.

Stein, S., J. M. Mills, and R. J. Geller (1981). Q^{-1} models from data space inversion of fundamental spheroidal mode attenuation measurements, *American Geophysical Union Monograph* (in press).

Sleep, N. H., R. J. Geller, and S. Stein (1981). A constraint on the earth's lateral heterogeneity from the scattering of spheroidal mode Q^{-1} measurements, *Bull. Seism. Soc. Am.* **71,** 183–198.

Department of Geological Sciences
Northwestern University
Evanston, Illinois 60201

Manuscript received June 26, 1980